Mathematical Modelling and Analysis
Volume 28, Issue 3, 487–508, 2023
https://doi.org/10.3846/mma.2023.17553

A Numerical Method for 3D Time-Dependent Maxwell's Equations in Axisymmetric Singular Domains with Arbitrary Data

Franck Assous[a] **and Irina Raichik**[b]

[a] *Ariel University*
40700 Ariel, Israel
[b] *Bar-Ilan University*
52900 Ramat-Gan, Israel
E-mail(*corresp.*): franckassous55@gmail.com
E-mail: irina.raichik@gmail.com

Received September 7, 2022; accepted June 12, 2023

Abstract. In this article, we propose to solve the three-dimensional time-dependent Maxwell equations in a singular axisymmetric domain with arbitrary data. Due to the axisymmetric assumption, the singular computational domain boils down to a subset of $\mathbb{R}^2$. However, the electromagnetic field and other vector quantities still belong to $\mathbb{R}^3$. Taking advantage that the domain is transformed into a two-dimensional one, by doing Fourier analysis in the third dimension, one arrives to a sequence of singular problems set in a 2D domain. The mathematical tools of such problems have been exposed in [4, 19]. Here, we derive a variational method from which we propose an original finite element numerical approach to solve the problem. Numerical experiments are also shown to illustrate that the method is able to capture the singular part of the solution. This approach can also be viewed as a generalization of the Singular Complement Method to three-dimensional problem.

Keywords: time-dependent Maxwell equations, Fourier analysis, singularities, axisymmetric geometry.

AMS Subject Classification: 65N30; 78M10; 35B65; 35L67.

1 Introduction

There is a need to simulate electromagnetic wave phenomena of increasing complexity, leading to the development of more general and efficient numerical

methods. Indeed, a significant number of engineering problems requiring to simulate numerically devices working with electromagnetic fields have come out.

This article is part of the efforts made in the framework of non-smooth problems, that are not necessarily convex curvilinear polyhedra. In these conditions, such domains may contain reentrant edges that generate singularities in Maxwell's equations solutions. In the same way, note that a change in the type of boundary conditions [23, 24] can also generate such singularities, even in a more regular geometry. From a more intuitive point of view, the term singularities means that such geometrical features can generate, in their vicinity, very strong electromagnetic fields, that have to be carefully handled and are often difficult to compute. Moreover, as shown in [5], the impossibility of correctly handling these singularities may have drastic consequences on the phenomenon one wants to model.

In this context, many methods have been proposed to compute the solution to the Maxwell equations. We can mention the edge finite element method, introduced by Nédélec [31, 32], that has demonstrated efficiency for the static and eigenvalue problems. More recently, discontinuous Galerkin method has been introduced [28] and have been extensively studied since then. In [15], Brenner et al. have also proposed an adaptive finite element method that works in dimension two.

On the other hand, it is interesting for some applications to have a continuous approximation of the solutions, that can capture both the curl and the divergence of the electromagnetic fields, for instance when coupling the Maxwell equations in other equations, like the Vlasov one, see [6]. But the latter works only in convex (curvilinear) polyhedra.

Indeed, when one solves Maxwell's equations in a non-convex domain with a continuous discretization, the discretized spaces are included in a closed, strict subspace of the space of real solutions, see the seminal work of [13,14] for theoretical proofs. Hence, one can not approximate the singular field without a special treatment, even for static problems [20]. For this reason, an ansatz like mesh refinement techniques fails. The Singular Complement Method proposed in [4, 5] is a way to overcome this difficulty by explicitly adding some adapted singular complements.

However, solving numerically three-dimensional boundary value problems in a non-convex domain is in substance different from the two-dimensional case and is often more difficult and more expensive. When it is possible, a convenient way to reduce the three-dimensional problem to two-dimensional equations, is to assume that the geometry is invariant by translation or by rotation. Assuming further that the data are also invariant, the problem can be reduced to a two-dimensional one. This approach has been widely used, even for singular problems, see for instance [4, 5, 20].

In this spirit, for an axisymmetric domain, the so-called Fourier Finite Element Method is an efficient way to solve problems in three-dimensional axisymmetric domains, even for other equations, see for instance [11] for Stokes equations. The method uses the Fourier expansion in one space direction associated to a finite element approach in the other two space dimensions, see

among others [16, 24, 26, 30] or [27] for interface problems.

In this paper, we also consider a geometrical reduction of Maxwell's equations in a singular axisymmetric geometry, in which the three-dimensional time-dependent Maxwell equations can be reformulated as geometrically simpler models. Essentially, this uses the fact that the azimuthal direction is orthogonal to the singularities and so does not "see them". Hence, it is worth to reduce the three dimensional problem to a series of two dimensional ones, that can be solved even if the geometry is singular.

More precisely, we consider the three-dimensional time-dependent Maxwell equations in a singular axisymmetric domain. Due to the axisymmetric assumption, the singular computational domain is reduced to a subset of $\mathbb{R}^2$. However, we assume that the data are *arbitrary*, namely not necessarily axisymmetric. Hence, the electromagnetic field and other vector quantities still belong to $\mathbb{R}^3$. Taking advantage that the domain is transformed into a two-dimensional one, by doing Fourier analysis in the third dimension, one arrives to a sequence of singular problems set in a 2D domain. We then derive a variational formulation from which we propose a finite element method to solve the problem and numerically compute the solution.

This paper is organized as follows: in a first section, we recall the Maxwell equations and their formulations in an axisymmetric domain. Then, we present the principle of the 2D space reduction, based on the use of a Fourier transform in θ. This reduces 3D Maxwell's equations to a series of 2D Maxwell's equations, depending on the Fourier variable k. This will allow us to compute the 3D solution by solving several 2D problems, each one depending on k. Even if the solution remains singular for each k in the 2D domain, we will be able to decompose it into a regular and a singular part (see Section 4). The regular part belongs to a regular space and will be computed by a standard finite element method. The singular part, that belongs to a finite-dimensional subspace, will be handled following the same principle as in [4]. This is the subject of Section 5. The numerical method to solve the time-dependent problem is developed in Section 6 for both electric and magnetic fields. In the Section 7, numerical examples are proposed to illustrate the feasibility of the method.

In the remainder of the article, we write vector fields or spaces with boldface. In a similar way, names of function spaces of scalar fields usually begin by an italic letter (for instance, $\mathbf{L}^2(\Omega) = L^2(\Omega)^3$ or $L^2(\Omega)^2$).

2 Geometry setting and Maxwell's equations

2.1 The Maxwell equations

In this article, we consider an axisymmetric bounded and simply connected Lipschitz domain Ω in $\mathbb{R}^3$. Its boundary is denoted by Γ and $\mathbf{n}$ is the unit outward normal to Γ. We also denote by c and ε_0 the speed of light and the dielectric permittivity respectively. Hence, the evolution of a time-dependent electromagnetic field $\mathbf{E}(\mathbf{x}, t), \mathbf{B}(\mathbf{x}, t)$ propagating in vacuum is governed by Maxwell's

equations:

$$\frac{\partial \mathbf{E}}{\partial t} - c^2 \mathbf{curl}\ \mathbf{B} = -\frac{1}{\varepsilon_0}\mathbf{J}, \tag{2.1}$$

$$\frac{\partial \mathbf{B}}{\partial t} + \mathbf{curl}\ \mathbf{E} = 0,$$

$$\text{div}\ \mathbf{E} = \frac{\rho}{\varepsilon_0}, \tag{2.2}$$

$$\text{div}\ \mathbf{B} = 0\,, \tag{2.3}$$

where $\rho(\mathbf{x}, t)$ and $\mathbf{J}(\mathbf{x}, t)$ are the charge and current densities, that depend on the space variable $\mathbf{x}$ and on the time variable t. As it well known, the divergence constraints (2.2)–(2.3) are satisfied at any time t if they are satisfied at the initial time $t = 0$, and provided that the charge conservation equation holds for the E-field. However, in the discrete case, these properties sometimes do not pass to the numerical approximation. We can deal with this problem by introducing the Lagrange multipliers of the constraints (2.2)–(2.3), as proposed in [6].

These equations are supplemented with appropriate boundary conditions. In this article, we assume that the boundary Γ is a perfect conductor, so that the electromagnetic field satisfies

$$\mathbf{E}(\mathbf{x}, t) \times \mathbf{n} = 0 \quad \text{and} \quad \mathbf{B}(\mathbf{x}, t) \cdot \mathbf{n} = 0 \quad \text{on the boundary } \Gamma\,, \tag{2.4}$$

but one can extend our results to the case of non homogeneous materials (see [22]), or impose a Silver-Müller absorbing boundary condition on a part of the boundary, see for instance [4, 5] or [10].

Remark 1. For the sake of simplicity, we only consider homogeneous materials. However, the case of non-homogeneous materials can be handled in a similar way, under the conditions that the decomposition into regular and singular parts (introduced in Section 4) can be performed. This is for example the case for several material media, with different constant dielectric permittivities and magnetic permeabilities, see for instance [7].

Last, initial conditions are provided, for instance at initial time $t = 0$

$$\mathbf{E}(\mathbf{x}, 0) = \mathbf{E}_0 \quad \text{and} \quad \mathbf{B}(\mathbf{x}, 0) = \mathbf{B}_0,$$

where $\mathbf{E}_0$ and $\mathbf{B}_0$ only depend on the variable $\mathbf{x}$ and satisfies the divergence conditions (2.2)–(2.3) and the boundary conditions (2.4). Existence and uniqueness of this problem is well known [29], and deeply studied for instance in [3].

2.2 Formulation in an axisymmetric domain

From now on, we assume that the domain Ω is an axisymmetric one, limited by the surface of revolution Γ. We denote by ω and γ_b their intersections with a meridian half-plane, as depicted in Figure 1.

The boundary $\partial\omega := \gamma$ corresponds to $\gamma_a \cup \gamma_b$, where either $\gamma_a = \emptyset$ when γ_b is a closed contour (i.e., Ω does not contain the axis) or γ_a is the segment of the

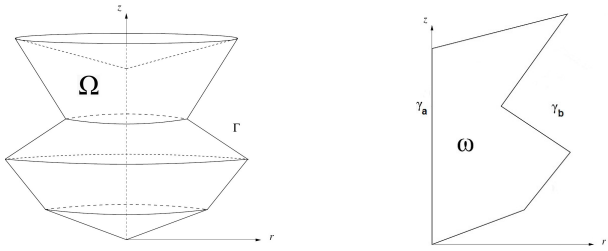

Figure 1. Example of 3D domain Ω, and its corresponding 2D intersection with meridian half-plane ω.

axis lying between the extremities of γ_b. The natural coordinates for this domain are the cylindrical coordinates (r, θ, z), with the basis vectors $(\mathbf{e}_r, \mathbf{e}_\theta, \mathbf{e}_z)$. A meridian half-plane is defined by the equation θ =constant, and (r, z) are Cartesian coordinates in this half-plane.

However, even if we assumed symmetry of revolution for the domain Ω, we *do not assumed* such a symmetry for the data. Consequently, the problem can not be reduced to a two-dimensional one by assuming that derivative with respect to the azimuthal variable θ vanishes, i.e. $\partial/\partial\theta = 0$, as made for example in [4]: we have to continue to deal with a three-dimensional problem.

Taking this remark into account, it is natural to rewrite the Maxwell equations (2.1)–(2.3) simply by replacing the operators div and **curl** by their cylindrical counterparts in the cylindrical coordinates (r, θ, z), defined by

$$\operatorname{div}\mathbf{u} = \frac{1}{r}\frac{\partial}{\partial r}(ru_r) + \frac{1}{r}\frac{\partial u_\theta}{\partial\theta} + \frac{\partial u_z}{\partial z},$$
$$\mathbf{curl}\,\mathbf{u} = \left(\frac{1}{r}\frac{\partial u_z}{\partial\theta} - \frac{\partial u_\theta}{\partial z}\right)\mathbf{e}_r + \left(\frac{\partial u_r}{\partial z} - \frac{\partial u_z}{\partial r}\right)\mathbf{e}_\theta + \frac{1}{r}\left(\frac{\partial}{\partial r}(ru_\theta) - \frac{\partial u_r}{\partial\theta}\right)\mathbf{e}_z.$$

Similarly, the gradient operator in cylindrical coordinates is expressed as

$$\mathbf{grad}\, f = \frac{\partial f}{\partial r}\mathbf{e}_r + \frac{1}{r}\frac{\partial f}{\partial\theta}\mathbf{e}_\theta + \frac{\partial f}{\partial z}\mathbf{e}_z.$$

Following [6], it is more efficient if one wishes to use nodal finite element methods, for instance for charge particle simulations as in the context of Vlasov-Maxwell computations, to eliminate the magnetic field $\mathbf{B}$ (respectively the electric field $\mathbf{E}$) from Equations (2.1)–(2.3). Maxwell's equations reduce to two second-order wave equations for each field separately:

$$\frac{\partial^2\mathbf{E}}{\partial t^2} + c^2\mathbf{curl}\,\mathbf{curl}\,\mathbf{E} = -\frac{1}{\varepsilon_0}\frac{\partial\mathbf{J}}{\partial t}, \tag{2.5}$$
$$\frac{\partial^2\mathbf{B}}{\partial t^2} + c^2\mathbf{curl}\,\mathbf{curl}\,\mathbf{B} = \frac{1}{\varepsilon_0}\mathbf{curl}\,\mathbf{J}\,, \tag{2.6}$$

the constraints equations, namely divergence and boundary conditions, still holding. Moreover, we have to add initial conditions for $\frac{\partial\mathbf{E}}{\partial t}$ and $\frac{\partial\mathbf{B}}{\partial t}$, since we

are dealing with a second order problem. We obtain them in a direct way from the Maxwell equations as

$$\frac{\partial \mathbf{E}}{\partial t}(t=0) = c^2 \mathbf{curl}\ \mathbf{B}_0 - \frac{1}{\varepsilon_0}\mathbf{J}(t=0)\,,$$
$$\frac{\partial \mathbf{B}}{\partial t}(t=0) = -\mathbf{curl}\ \mathbf{E}_0\,.$$

One can also had terms related to the divergence of the fields, yielding the so-called augmented formulations:

$$\frac{\partial^2 \mathbf{E}}{\partial t^2} + c^2(\mathbf{curl}\,\mathbf{curl}\,\mathbf{E} - \mathbf{grad}\,\mathrm{div}\,\mathbf{E}) = -\frac{1}{\varepsilon_0}\frac{\partial \mathbf{J}}{\partial t} - \frac{c^2}{\varepsilon_0}\mathbf{grad}\,\rho, \quad (2.7)$$

$$\frac{\partial^2 \mathbf{B}}{\partial t^2} + c^2(\mathbf{curl}\,\mathbf{curl}\,\mathbf{B} - \mathbf{grad}\,\mathrm{div}\,\mathbf{B}) = \frac{1}{\varepsilon_0}\mathbf{curl}\,\mathbf{J}\,, \quad (2.8)$$

supplemented with initial and boundary conditions.

2.3 Variational formulations in 3D

Let us now introduce the variational formulations of the problem, which can be applied for a given (convex or not) domain Ω. For this purpose, we define the usual function spaces with classical notations. In the text, names of function spaces of scalar fields usually begin by an italic letter, whereas they begin by a bold letter for spaces of vector fields (for instance, $\mathbf{L}^2(\Omega) = L^2(\Omega)^3$ or $L^2(\Omega)^2$). The usual norm and scalar product of $\mathbf{L}^2(\Omega)$ are denoted by $\|\cdot\|_0$ and $(\cdot,\cdot)$ respectively. We shall also need to use the following Sobolev spaces and norms

$$\mathbf{H}(\mathbf{curl}\,,\Omega) = \{\mathbf{v} \in \mathbf{L}^2(\Omega),\ \mathbf{curl}\,\mathbf{v} \in \mathbf{L}^2(\Omega)\}\,, \quad \|\mathbf{v}\|^2_{\mathbf{curl}} = \|\mathbf{v}\|^2_0 + \|\mathbf{curl}\,\mathbf{v}\|^2_0\,,$$
$$\mathbf{H}(\mathrm{div}\,,\Omega) = \{\mathbf{v} \in \mathbf{L}^2(\Omega),\ \mathrm{div}\,\mathbf{v} \in L^2(\Omega)\}\,, \quad \|\mathbf{v}\|^2_{\mathrm{div}} = \|\mathbf{v}\|^2_0 + \|\mathrm{div}\,\mathbf{v}\|^2_0\,,$$
$$\mathbf{H}^1(\Omega) = \{\mathbf{v} \in \mathbf{L}^2(\Omega),\ \mathbf{grad}\,\mathbf{v} \in \mathbf{L}^2(\Omega)\}\,, \quad \|\mathbf{v}\|^2_1 = \|\mathbf{v}\|^2_0 + \|\mathbf{grad}\,\mathbf{v}\|^2_0\,.$$

We introduce analogously the spaces for the **curl** and div operators

$$\mathbf{H}_0(\mathbf{curl}\,;\Omega) = \{\mathbf{v} \in \mathbf{H}(\mathbf{curl}\,;\Omega) : \mathbf{v}\times\mathbf{n}|_\Gamma = 0\}\,,$$
$$\mathbf{H}_0(\mathrm{div}\,;\Omega) = \{\mathbf{v} \in \mathbf{H}(\mathrm{div}\,;\Omega) : \mathbf{v}\cdot\mathbf{n}|_\Gamma = 0\}\,,$$

so that electric and magnetic field naturally belongs to the spaces

$$\mathbf{X}(\Omega) = \mathbf{H}_0(\mathbf{curl}\,;\Omega) \cap \mathbf{H}(\mathrm{div}\,\mathbf{v};\Omega)\,,\quad \mathbf{Y}(\Omega) = \mathbf{H}(\mathbf{curl}\,;\Omega) \cap \mathbf{H}_0(\mathrm{div}\,\mathbf{v};\Omega)\,.$$

In practice, we use a result from [21,34], that claims that the spaces $\mathbf{X}(\Omega)$ and $\mathbf{Y}(\Omega)$ are compactly embedded in $\mathbf{L}^2(\Omega)$. In these conditions, for a connected boundary Γ, one can equivalently define a scalar product and the related norm on $\mathbf{X}(\Omega)$ (respectively on $\mathbf{Y}(\Omega)$) by

$$a(\mathbf{u},\mathbf{v}) := (\mathbf{curl}\,\mathbf{u},\mathbf{curl}\,\mathbf{v}) + (\mathrm{div}\,\mathbf{u},\mathrm{div}\,\mathbf{v})\,,\quad \|\mathbf{u}\|_{\mathbf{X}} = \|\mathbf{u}\|_{\mathbf{Y}} := a(\mathbf{u},\mathbf{v})^{1/2}\,.$$

In other words, this means that the $\mathbf{L}^2$-norm is uniformly bounded by the X and the Y norm, for elements belonging to $\mathbf{X}(\Omega)$ or $\mathbf{Y}(\Omega)$. This is the so-called Weber inequality, that basically expresses that in $\mathbf{X}(\Omega)$ or in $\mathbf{Y}(\Omega)$,

the semi-norm $\mathbf{u} \longrightarrow (\|\mathbf{curl}\,\mathbf{u}\|_0^2 + \|\mathrm{div}\,\mathbf{u}\|_0^2)^{1/2}$ is a norm equivalent to the canonical one.

We are now in a position to derive the (augmented) variational formulations associated to problems (2.5)–(2.6) or (2.7)–(2.8). Let us derive it from the first one. As usual, we first take the dot product of Equations (2.5) and (2.6) by $\mathbf{F} \in \mathbf{X}(\Omega)$ and $\mathbf{C} \in \mathbf{Y}(\Omega)$, and integrate them over Ω. We then use a Green formula and add the variational form of the divergence equation for $\mathbf{E}$ and $\mathbf{B}$ respectively, to finally obtain the formulation for the vector wave equation (2.5)–(2.6):
Find $\boldsymbol{E}(t) \in \boldsymbol{X}(\Omega)$ *and* $\boldsymbol{B}(t) \in \boldsymbol{Y}(\Omega)$ such that:

$$\frac{d^2}{dt^2}(\mathbf{E}(t),\mathbf{F}) + c^2\, a(\mathbf{E}(t),\mathbf{F}) = -\frac{1}{\varepsilon_0}\left(\frac{\partial \mathbf{J}}{\partial t},\mathbf{F}\right) + \frac{1}{\varepsilon_0}(\rho, \mathrm{div}\,\mathbf{F}), \forall \mathbf{F} \in \mathbf{X}(\Omega),$$
$$\frac{d^2}{dt^2}(\mathbf{B}(t),\mathbf{C}) + c^2\, a(\mathbf{B}(t),\mathbf{C}) = \frac{1}{\varepsilon_0}(\mathbf{curl}\,\mathbf{J},\mathbf{C}), \forall \mathbf{C} \in \mathbf{Y}(\Omega).$$

This formulation can be similarly derived from problem (2.7)–(2.8). Theoretical results about these formulations have been established for several years now, see for instance a summary in [3].

3 Two-dimensional space reduction

As the data we consider are not axisymmetric, one can not use that all derivatives in the θ direction vanish. This means that one can not perform $\partial/\partial\theta = 0$ to reduce the $3D$ space problem to a $2D$ space one. However, one can use the cylindrical symmetry of the domain Ω to characterize the scalar and vector fields defined on it through their Fourier series in θ, the coefficients of which being functions defined on ω.

Note that such a technique together with the Fourier-Laplace transform is also used for stability analysis of numerical schemes [17] solving Maxwell equations. Moreover, since the time dependent part of the problem is not explicitly involved in this dimension reduction, we do not mention the time variable in the Fourier series, which can be easily added. For example, we will consider, for a given function $w(r,\theta,z)$ or for a vector field $\mathbf{w}(r,\theta,z)$, the following Fourier expansions

$$w(r,\theta,z) = \frac{1}{\sqrt{2\pi}}\sum_{k\in\mathbb{Z}} w^k(r,z)\, e^{ik\theta}, \quad \mathbf{w}(r,\theta,z) = \frac{1}{\sqrt{2\pi}}\sum_{k\in\mathbb{Z}} \mathbf{w}^k(r,z)\, e^{ik\theta},$$

and the related truncated Fourier expansions of w and $\mathbf{w}$ at order N, that is

$$w^{[N]}(r,\theta,z) = \frac{1}{\sqrt{2\pi}}\sum_{k=-N}^{N} w^k(r,z)\, e^{ik\theta}, \ \mathbf{w}^{[N]}(r,\theta,z) = \frac{1}{\sqrt{2\pi}}\sum_{k=-N}^{N} \mathbf{w}^k(r,z)\, e^{ik\theta}. \tag{3.1}$$

In the sequel, we will also need the following weighted Lebesgue space

$$L^2_r(\omega) := \left\{ w \text{ measurable on } \omega : \iint_\omega |w(r,z)|^2\, r dr dz < \infty \right\}$$

that will be the space of Fourier coefficients (at all modes) of functions in $\mathbf{L}^2(\Omega)$. At the same time, let us also define the space of relevant Fourier coefficients for the electromagnetic fields. It is easy to check that, for $w \in H^1(\Omega)$, resp. $w \in L^2(\Omega)$ such that $\Delta w \in L^2(\Omega)$, it holds

$$\mathbf{grad}\, w = \frac{1}{\sqrt{2\pi}} \sum_{k\in\mathbb{Z}} \mathbf{grad}_k w^k e^{ik\theta}, \text{ resp. } \Delta w = \frac{1}{\sqrt{2\pi}} \sum_{k\in\mathbb{Z}} \Delta_k w^k e^{ik\theta},$$

while for $\mathbf{w} \in \mathbf{H}(\mathrm{div}\,;\Omega)$, resp. $\mathbf{H}(\mathbf{curl}\,;\Omega)$, one has

$$\mathrm{div}\, \mathbf{w} = \frac{1}{\sqrt{2\pi}} \sum_{k\in\mathbb{Z}} \mathrm{div}_k \mathbf{w}^k e^{ik\theta} \text{ resp. } \mathbf{curl}\, \mathbf{w} = \frac{1}{\sqrt{2\pi}} \sum_{k\in\mathbb{Z}} \mathbf{curl}_k \mathbf{w}^k e^{ik\theta}.$$

In the expressions above, the operators for each mode k are defined as

$$\mathbf{grad}_k := \frac{\partial w}{\partial r}\mathbf{e}_r + \frac{ik}{r} w \mathbf{e}_\theta + \frac{\partial w}{\partial z}\mathbf{e}_z; \quad \Delta_k w := \frac{1}{r}\frac{\partial}{\partial r}\left(r\frac{\partial w}{\partial r}\right) - \frac{k^2}{r^2}w + \frac{\partial^2 w}{\partial z^2};$$
$$\mathrm{div}_k \mathbf{w} := \frac{1}{r}\frac{\partial (r w_r)}{\partial r} + \frac{ik}{r} w_\theta + \frac{\partial w_z}{\partial z}; \quad (\mathbf{curl}_k \mathbf{w})_r := \frac{ik}{r} w_z - \frac{\partial w_\theta}{\partial z};$$
$$(\mathbf{curl}_k \mathbf{w})_\theta := \frac{\partial w_r}{\partial z} - \frac{\partial w_z}{\partial r}; \quad (\mathbf{curl}_k \mathbf{w})_z := \frac{1}{r}\left(\frac{\partial (r w_\theta)}{\partial r} - ik w_r\right).$$

Concerning the regularity of w and of the components of $\mathbf{w}$, as explained in [12], it only depends on the regularity of the Fourier components of w^k and $\mathbf{w}^k$, for $k \in \mathbb{Z}$. As a consequence, a function $\mathbf{v}$ belongs to $\mathbf{X}(\Omega)$ if and only if, for all $k \in \mathbb{Z}$, its Fourier coefficients $\mathbf{v}^k$ belong to the space $\mathbf{X}_{(k)}(\omega)$ defined by

$$\mathbf{X}_{(k)}(\omega) = \{\mathbf{v}^k \in \mathbf{L}^2_r(\omega),\ \mathbf{curl}_k \mathbf{v}^k \in \mathbf{L}^2_r(\omega), \mathrm{div}_k \mathbf{v}^k \in \mathbf{L}^2_r(\omega), \mathbf{v}^k \times \mathbf{n}_{|\gamma_b} = 0\}.$$

In a similar way, one introduces the space $\mathbf{Y}_{(k)}(\omega)$ for the Fourier coefficients of elements of $\mathbf{Y}(\Omega)$, namely

$$\mathbf{Y}_{(k)}(\omega) = \{\mathbf{v}^k \in \mathbf{L}^2_r(\omega),\ \mathbf{curl}_k \mathbf{v}^k \in \mathbf{L}^2_r(\omega), \mathrm{div}_k \mathbf{v}^k \in \mathbf{L}^2_r(\omega), \mathbf{v}^k \cdot \mathbf{n}_{|\gamma_b = 0}\}.$$

Let us recall an important and useful property concerning these spaces, proved in [19] (see also [18] for the Poisson problem), that will be used throughout the numerical method derived in the next sections. We have

Proposition 1. *The spaces $\boldsymbol{X}_{(k)}(\omega)$ and $\boldsymbol{Y}_{(k)}(\omega)$ are independent of k, for $|k| \geq 2$.*

This property will allow us to compute the singular subspaces only for the modes $|k| \leq 2$, while the modes ± 2 will be use to compute all the higher modes $|k| > 2$.

3.1 Variational formulation in 2D for each k

We now apply the principle of dimension reduction described above to reduce the 3D equations to a series of 2D formulations, the solutions of which are the Fourier coefficients $(\mathbf{E}_k, \mathbf{B}_k)$, for each mode k.

More precisely, one uses the linearity of the Maxwell equations together with the orthogonality of the different Fourier modes in $L^2(\omega)$. This implies that the Fourier coefficients $(\mathbf{E}_k, \mathbf{B}_k)$ of the 3D electromagnetic field $(\mathbf{E}, \mathbf{B})$ is solution to similar formulations set in the 2D domain ω, with the operators $\mathbf{curl}_k$ and div_k. For convenience, let us introduce the operator $a_k(\cdot,\cdot)$

$$a_k(\mathbf{u}, \mathbf{v}) = (\mathbf{curl}_k \mathbf{u}, \mathbf{curl}_k \mathbf{v}) + (\mathrm{div}_k \mathbf{u}, \mathrm{div}_k \mathbf{v}). \tag{3.2}$$

We get that each mode $\mathbf{E}^k$ is solution to the following variational formulation:
Find $\boldsymbol{E}^k(t) \in \boldsymbol{X}_{(k)}(\omega)$ *such that, for all* $\boldsymbol{F} \in \boldsymbol{X}_{(k)}(\omega)$*:*

$$\frac{d^2}{dt^2}\left(\mathbf{E}^k(t), \mathbf{F}\right) + c^2\, a_k\left(\mathbf{E}^k(t), \mathbf{F}\right) = -\frac{1}{\varepsilon_0}\left(\partial_t \mathbf{J}^k, \mathbf{F}\right) + \frac{1}{\varepsilon_0}\left(\rho^k, \mathrm{div}_k \mathbf{F}\right), \tag{3.3}$$

where ρ^k and $\mathbf{J}^k$ denote the Fourier coefficients of the charge and current density ρ and $\mathbf{J}$ respectively, that depend (in space) only on (r, z).

In the same way, for the magnetic field $\mathbf{B}(t)$, one gets that its Fourier coefficients $\mathbf{B}_k(t)$ verify the variational formulation, for each mode k:
Find $\boldsymbol{B}^k(t) \in \boldsymbol{Y}_{(k)}(\omega)$ *such that, for all* $\boldsymbol{C} \in \boldsymbol{Y}_{(k)}(\omega)$*:*

$$\frac{d^2}{dt^2}\left(\mathbf{B}^k(t), \mathbf{C}\right) + c^2\, a_k\left(\mathbf{B}^k(t), \mathbf{C}\right) = \frac{1}{\varepsilon_0}\left(\mathbf{curl}_k \mathbf{J}^k, \mathbf{C}\right). \tag{3.4}$$

Now, concerning the the truncation error of the Fourier expansion, a mathematical analysis has been proposed in [19, 33], the interested reader is referred to these references. For short, it is proved there that the truncated solution $\mathbf{E}^{[N]}$, as defined in (3.1), converges toward $\mathbf{E}$ as N^{-2s}, the value of $s > 1/2$ depending on the regularity of $\mathbf{E}(t)$ and $\frac{\partial \mathbf{E}(t)}{\partial t}$. Similar results have been proved for the convergence of $\mathbf{B}^{[N]}$ toward $\mathbf{B}$.

4 Decomposition in regular and singular parts

So far, as for instance in [30], we have considered a geometrical reduction of Maxwell's equations in an axisymmetric geometry, in which the three-dimensional Maxwell equations can be reformulated as a geometrically simpler model. However, the geometrical singularities remain in the two-dimensional domain ω (see Figure 1), and we have now to deal with. For our purpose here, we rely on theoretical results proved in [1], for the case $k = 0$, namely the full axisymmetric case, and in [19] for the general case. For the self-content of the article, we briefly recall, without proof, some useful results that help to understand the construction of the numerical method.

We first consider, for each mode k, the weighted Sobolev space $\mathbf{H}^1_r(\omega)$ that contains functions $\mathbf{v}^k \in \mathbf{L}^2_r(\omega)$ such that $\mathbf{grad}_k \mathbf{v}^k \in \mathbf{L}^2_r(\omega)$. Now, we introduce, for each Fourier mode k, the regular subspaces $\mathbf{X}^R_{(k)}(\omega)$ and $\mathbf{Y}^R_{(k)}(\omega)$, defined by:

$$\mathbf{X}^R_{(k)}(\omega) := \mathbf{X}_{(k)}(\omega) \cap \mathbf{H}^1_r(\omega) \text{ and } \mathbf{Y}^R_{(k)}(\omega) := \mathbf{Y}_{(k)}(\omega) \cap \mathbf{H}^1_r(\omega).$$

These subspaces are regular, in the sense that they coincide to the spaces of solutions in the case of a regular domain. Using now that $\mathbf{X}^R_{(k)}(\omega)$ and

$\mathbf{Y}^R_{(k)}(\omega)$ are closed subspaces of $\mathbf{X}_{(k)}(\omega)$ and $\mathbf{Y}_{(k)}(\omega)$ respectively, we deduce the following decomposition

$$\mathbf{X}_{(k)}(\omega) = \mathbf{X}^R_{(k)}(\omega) \oplus \mathbf{X}^S_{(k)}(\omega) \qquad \text{and} \qquad \mathbf{Y}_{(k)}(\omega) = \mathbf{Y}^R_{(k)}(\omega) \oplus \mathbf{Y}^S_{(k)}(\omega)\,,$$

where $\mathbf{X}^S_{(k)}(\omega)$ and $\mathbf{Y}^S_{(k)}(\omega)$ are singular subspaces, equal to $\{0\}$ if the domain Ω (or equivalently ω) is regular.

As a second step, we have to characterize these singular spaces. For a two-dimensional axisymmetric domain, it was also proved (see the references above), that they are of finite dimension, the dimension of which depending on the number N_S of singularities in the domain ω. More precisely, we have the following result (see Figure 2).

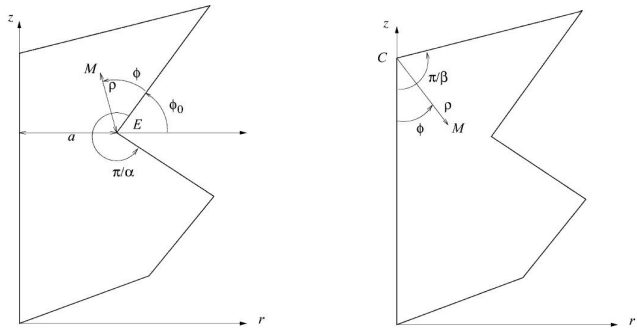

Figure 2. Local coordinates near a reentrant edge (left) and a conical point (right). For clarity, the index $_j$ has been dropped.

Proposition 2. *The singular spaces $\boldsymbol{X}^S_{(k)}(\omega)$ and $\boldsymbol{Y}^S_{(k)}(\omega)$ are of finite dimension, namely*

- *For $k = 0$,*

$$\dim \boldsymbol{Y}^S_{(k)}(\omega) := N_B = \text{ number of reentrant edges,}$$
$$\dim \boldsymbol{X}^S_{(k)}(\omega) := N_E = N_B + \text{ number of conical points with vertex angle } > \pi/\beta^\star,\ \beta^\star \simeq 1.3731.$$

- *For $k \neq 0$,*

$$\dim \boldsymbol{Y}^S_{(k)}(\omega) := N_B = \dim \boldsymbol{X}^S_{(k)}(\omega) := N_E = \text{number of reentrant edges.}$$

Resulting from these properties, one can decompose, for each mode k, the electromagnetic field $\mathbf{E}^k, \mathbf{B}^k$ into a regular part and a singular one, namely

$$\mathbf{E}^k(t) = \mathbf{E}^k_R(t) + \mathbf{E}^k_S(t), \quad \mathbf{B}^k(t) = \mathbf{B}^k_R(t) + \mathbf{B}^k_S(t)\,. \tag{4.1}$$

Moreover, since the singular spaces are of finite dimension, one can introduce their respective basis $(\mathbf{x}^k_{S,j})_{j=1,N_E}$ and $(\mathbf{y}^k_{S,j})_{j=1,N_B}$ for a given Fourier mode k.

Using now that these basis are time independent, one can express the singular parts $\mathbf{E}_S^k(t)$ and $\mathbf{B}_S^k(t)$ as

$$\mathbf{E}_S^k(t) = \sum_{j=1}^{N_E} \mu_{E,j}^k(t)\mathbf{x}_{S,j}^k, \qquad \mathbf{B}_S^k(t) = \sum_{j=1}^{N_B} \mu_{B,j}^k(t)\mathbf{y}_{S,j}^k\,,$$

where $\mu_{E,j}^k(t)$ and $\mu_{B,j}^k(t)$ are smooth functions in time (at least continuous, cf [2]). As a consequence, the decomposition (4.1) of the electromagnetic, that will be useful for the numerical method, can be finally expressed, for each k,

$$\mathbf{E}^k(t) = \mathbf{E}_R^k(t) \oplus \sum_{j=1}^{j=N_E} \mu_{E,j}^k(t)\mathbf{x}_{S,j}^k, \quad \mathbf{B}^k(t) = \mathbf{B}_R^k(t) \oplus \sum_{j=1}^{j=N_B} \mu_{B,j}^k(t)\mathbf{y}_{S,j}^k\,. \tag{4.2}$$

The last part consists in characterizing and computing the static basis $\mathbf{x}_{S,j}^k$ and $\mathbf{y}_{S,j}^k$. From a numerical point of view, remark that, due to the Proposition 1, it will be sufficient to compute them only for $k = -1, 0, 1, 2$. As these basis are not time-dependent, the computations will be carried out only once as an initialization procedure.

5 Computation of singular basis, for $|k| \leq 2$

In this section, we briefly recall for completeness, the method used to compute the singular basis $\mathbf{x}_{S,j}^k, 1 \leq j \leq N_E$ and $\mathbf{y}_{S,j}^k, 1 \leq j \leq N_B$. Details can be found in [9]. For each Fourier mode indexed by $k \in \mathbb{Z}$, and for a given singularity indexed by j, $1 \leq j \leq N_B$, the electric and magnetic singular basis $\mathbf{x}_{S,j}^k$ and $\mathbf{y}_{S,j}^k$ solve respectively the following variational formulation

$$\begin{cases} a_k\left(\mathbf{x}_{S,j}^k, \mathbf{v}\right) = 0, \ \forall \mathbf{v} \in \mathbf{X}_{(k)}^S(\omega), \\ \mathbf{x}_{S,j}^k \times \mathbf{n}|_{\gamma_b} = 0, \\ \mathbf{x}_{S,j}^k \cdot \mathbf{n}|_{\gamma_a} = 0, \end{cases} \qquad \begin{cases} a_k\left(\mathbf{y}_{S,j}^k, \mathbf{v}\right) = 0, \ \ \forall \mathbf{v} \in \mathbf{Y}_{(k)}^S(\omega), \\ \mathbf{y}_{S,j}^k \cdot \mathbf{n}|_{\gamma} = 0, \ \ \gamma := \gamma_b \cup \gamma_a\,. \end{cases} \tag{5.1}$$

These problems are obviously singular in the two-dimensional domain ω, in the sense that an attempt to solve them by a classical finite element method will give zero as a solution. However, the singular basis $\mathbf{x}_{S,j}^k$ and $\mathbf{y}_{S,j}^k$ computed in this way are by construction orthogonal to any element of $\mathbf{X}_{(k)}^R(\omega)$ and $\mathbf{Y}_{(k)}^R(\omega)$ respectively. This property will be useful to simplify the time-dependent formulations in Section 6.

Following the idea proposed in the full axisymmetric case [4], we introduce $\mathbf{S}_j^X$ (respectively $\mathbf{S}_j^Y$), the *principal part* of the singularity j, defined as the part that makes $\mathbf{x}_{S,j}^k$ (respectively $\mathbf{y}_{S,j}^k$) singular, and does not depend on the Fourier mode k (see [2, 3, 19]), that is,

$$\mathbf{x}_{S,j}^k = \mathbf{x}_{S,j,reg}^k + \mathbf{S}_j^X \quad \text{and} \quad \mathbf{y}_{S,j}^k = \mathbf{y}_{S,j,reg}^k + \mathbf{S}_j^Y\,.$$

Above, $\mathbf{x}_{S,j,reg}^k$ and $\mathbf{y}_{S,j,reg}^k$ denote a *regular part* of $\mathbf{x}_{S,j}^k$ and $\mathbf{y}_{S,j}^k$ respectively, that can be computed by a classical finite element method.

Considering the neighborhood of a reentrant edge E_j for a given j, we use the notations of Figure 2-left: in particular, (ρ, ϕ) denotes the local polar coordinates centered at the reentrant edge E_j, the corresponding angle being called π/α, $1/2 < \alpha < 1$, ϕ_0 being the angle between the r-axis and the origin of ϕ. For the conical point C, (ρ, ϕ) are the local polar coordinates centered at this point, with the origin of ϕ on the z-axis. Hence, the principal part can be expressed, for the electric and magnetic case respectively

$$\mathbf{S}_j^X = -\frac{r_j}{a_j}\alpha_j \rho^{\alpha_j - 1} \begin{pmatrix} \sin((\alpha_j - 1)\phi_j - \phi_{j,0}) \\ 0 \\ \cos((\alpha_j - 1)\phi_j - \phi_{j,0}) \end{pmatrix},$$

$$\mathbf{S}_j^Y = -\frac{r_j}{a_j}\alpha_j \rho^{\alpha_j - 1} \begin{pmatrix} \cos\left((\alpha_j - 1)\,\phi_j - \phi_{j,0}\right) \\ 0 \\ -\sin\left((\alpha_j - 1)\,\phi_j - \phi_{j,0}\right) \end{pmatrix},$$

the difference between the two expressions arising from the boundary conditions. Above, the term r_j/a_j helps us to impose the boundary condition on the axis $r = 0$, and can be viewed as a well-adapted cut-off function.
Note, that in the electric case only, and for the particular case $k = 0$ corresponding to the full axisymmetric case, there exists an additional conical singularity (C in Figure 2) in the neighborhood of a conical vertex with an aperture π/β greater than $\pi/\beta^\star$ for $\beta^\star \simeq 1.3731$. In the magnetic case, there is no conical singularity. Details can be found in [2]. Using these results, one computes the regular part of the singular electric basis $\mathbf{x}_{S,j,reg}^k$ by solving the variational formulation, for each j,

$$\begin{cases} a_k\left(\mathbf{x}_{S,j,reg}^k, \mathbf{v}\right) = -a_k\left(\mathbf{S}_j^X, \mathbf{v}\right) \quad \forall \mathbf{v} \in \mathbf{X}_{(k)}^R(\omega), \\ \mathbf{x}_{S,j,reg}^k \times \mathbf{n}|_{\gamma_b} = -\mathbf{S}_j^X \times \mathbf{n}|_{\gamma_b}, \\ \mathbf{x}_{S,j,reg}^k \cdot \mathbf{n}|_{\gamma_a} = 0, \end{cases}$$

and similarly for the singular magnetic basis $\mathbf{y}_{S,j,reg}^k$

$$\begin{cases} a_k\left(\mathbf{y}_{S,j,reg}^k, \mathbf{v}\right) = -a_k\left(\mathbf{S}_j^Y, \mathbf{v}\right) \quad \forall \mathbf{v} \in \mathbf{Y}_{(k)}^R(\omega), \\ \mathbf{y}_{S,reg}^k \cdot \mathbf{n}|_{\gamma} = -\mathbf{S}_j^Y \cdot \mathbf{n}|_{\gamma}. \end{cases}$$

Note that the right-hand side of these equations, in both electric and magnetic cases, can be obtained by computing the analytic expressions of $\mathbf{curl}\,{}_k\mathbf{S}_j^X$ and $\mathrm{div}\,{}_k\mathbf{S}_j^X$, involved in $a_k\left(\mathbf{S}_j^X, \mathbf{v}\right)$, and the same for the magnetic case, replacing $\mathbf{S}_j^X$ by $\mathbf{S}_j^Y$, see details in [9].

6 Solving the time-dependent problem

In what follows, we first present the case of the magnetic field formulation. The electric field formulation is similar and will be briefly exposed later.

For this purpose, we consider the variational formulation (3.4), in which we substitute the decomposition of the magnetic field (4.2) in regular and singular

parts. Using that the singular basis $\mathbf{y}_{S,j}^k$ are time-independent, and denoting by $''$ the second derivative in time, we get

$$\frac{d^2}{dt^2}\left(\mathbf{B}_R^k(t),\mathbf{C}\right)+\sum_{j=1}^{N_B}(\mu_{B,j}^k)''\left(\mathbf{y}_{S,j}^k,\mathbf{C}\right)+c^2\,a_k\left(\mathbf{B}_R^k(t),\mathbf{C}\right)$$
$$+c^2\sum_{j=1}^{N_B}\mu_{B,j}^k(t)\,a_k\left(\mathbf{y}_{S,j}^k,\mathbf{C}\right)=\frac{1}{\varepsilon_0}\left(\mathbf{curl}\,{}_k\mathbf{J}^k,\mathbf{C}\right),\forall\mathbf{C}\in\mathbf{Y}_{(k)}^R(\omega)\,.$$

In addition, we add to the space of test functions $\mathbf{Y}_{(k)}^R(\omega)$ the functions $(\mathbf{y}_{S,j}^k)_{j=1,N_B}$. This yields the N_B additional equations $(1\le i\le N_B)$

$$\frac{d^2}{dt^2}\left(\mathbf{B}_R^k(t),\mathbf{y}_{S,i}^k\right)+\sum_{j=1}^{N_B}(\mu_{B,j}^k)''\left(\mathbf{y}_{S,j}^k,\mathbf{y}_{S,i}^k\right)+c^2\,a_k\left(\mathbf{B}_R^k(t),\mathbf{y}_{S,i}^k\right)$$
$$+c^2\sum_{j=1}^{N_B}\mu_{B,j}^k(t)\,a_k\left(\mathbf{y}_{S,j}^k,\mathbf{y}_{S,i}^k\right)=\frac{1}{\varepsilon_0}\left(\mathbf{curl}\,{}_k\mathbf{J}^k,\mathbf{y}_{S,i}^k\right),\forall\mathbf{y}_{S,i}^k\in\mathbf{Y}_{(k)}^S(\omega).$$

Moreover, using the orthogonality for each k of $\mathbf{Y}_{(k)}^R(\omega)$ and $\mathbf{Y}_{(k)}^S(\omega)$ with respect to the equivalent scalar product $a_k(\cdot,\cdot)$ defined by (3.2), as recalled in (5.1), we can eliminate the corresponding terms in the formulations above. This variational formulation is finally expressed as

Find $(\boldsymbol{B}_R^k,\boldsymbol{\mu}_B^k)\in\boldsymbol{Y}_{(k)}^R(\omega)\times\mathbb{R}^{N_B}$ *such that*

$$\begin{cases}\left(\frac{\partial^2\mathbf{B}_R^k(t)}{\partial t^2},\mathbf{C}\right)+\sum_{j=1}^{N_B}(\mu_{B,j}^k)''\left(\mathbf{y}_{S,j}^k,\mathbf{C}\right)+c^2\,a_k\left(\mathbf{B}_R^k(t),\mathbf{C}\right)\\ \quad=\frac{1}{\varepsilon_0}\left(\mathbf{curl}\,{}_k\mathbf{J}^k,\mathbf{C}\right),\quad\forall\mathbf{C}\in\mathbf{Y}_{(k)}^R(\omega),\\ \left(\frac{\partial^2\mathbf{B}_R^k(t)}{\partial t^2},\mathbf{y}_{S,i}^k\right)+\sum_{j=1}^{N_B}(\mu_{B,j}^k)''\left(\mathbf{y}_{S,j}^k,\mathbf{y}_{S,i}^k\right)+c^2\sum_{j=1}^{N_B}\mu_{B,j}^k(t)\,a_k\left(\mathbf{y}_{S,j}^k,\mathbf{y}_{S,i}^k\right)\\ \quad=\frac{1}{\varepsilon_0}\left(\mathbf{curl}\,{}_k\mathbf{J}^k,\mathbf{y}_{S,i}^k\right),\quad\forall\mathbf{y}_{S,i}^k\in\mathbf{Y}_{(k)}^S(\omega).\end{cases}\tag{6.1}$$

From a computational point of view, it is worth to rewrite the bilinear form $a_k(\cdot,\cdot)$ involved above, depending on the values of k. Performing a simple integration by parts shows that

$$a_k(\mathbf{u},\mathbf{v})=a_0(\mathbf{u}_m,\mathbf{v}_m)+k^2\left(\frac{\mathbf{u}_m}{r},\frac{\mathbf{v}_m}{r}\right)+(\mathbf{curl}\,u_\theta,\mathbf{curl}\,v_\theta)+k^2\left(\frac{u_\theta}{r},\frac{v_\theta}{r}\right)$$
$$+\imath kB(\mathbf{u},\mathbf{v})+\imath kC(\mathbf{u},\mathbf{v}),$$

where $a_0(\cdot,\cdot)$ denotes the operator $a_k(\cdot,\cdot)$ for $k=0$ (namely in the "full" axisymmetric case), $\mathbf{u}_m:=(u_r,u_z)$ and the vector **curl** of a scalar field w is defined by

$$\mathbf{curl}\,w:=-\partial_z w\mathbf{e}_r+r^{-1}\partial_r(rw)\,\mathbf{e}_z\,.$$

In addition, the two bilinear forms $B(\mathbf{u},\mathbf{v})$ and $C(\mathbf{u},\mathbf{v})$ are defined by

$$B(\mathbf{u},\mathbf{v}) := \int_{\gamma_b} (\mathbf{u}_m \cdot \mathbf{n})\,\bar{v}_\theta - u_\theta\,(\bar{\mathbf{v}}_m \cdot \mathbf{n})\,d\gamma$$
$$C(\mathbf{u},\mathbf{v}) := \int\int_{\omega} 2\,(u_\theta \bar{v}_r - u_r \bar{v}_\theta)\,\frac{d\omega}{r}\,.$$

Note that the term $B(\mathbf{u},\mathbf{v})$ vanishes as soon $\mathbf{u}\cdot\mathbf{n} = \mathbf{v}\cdot\mathbf{n} = 0$, that is the case for the magnetic field, due to the perfect conductor boundary condition. The same will be also true if $\mathbf{u}\times\mathbf{n} = \mathbf{v}\times\mathbf{n} = 0$, that will be the case for the electric field. In addition, the term $C(\mathbf{u},\mathbf{v})$ is not singular despite the presence of $1/r$ in the integral. Indeed, only on the boundary γ_a one may have $r = 0$, but $u_\theta = v_\theta = 0$ (that is in practice B_θ^k or E_θ^k for the electric case) due the symmetry condition on the axis γ_a.

Starting from this variational formulation, we are now ready to derive a finite element approximation. We first introduce a finite element partition of the domain ω, and we denote by $\mathcal{T}_h$ the mesh of ω made of triangles K_h, h being the size of the mesh. We actually used the P_2 finite element approximation, so that the approximation space for the vector fields is made of functions which are component-wise P_2-conforming on the triangulation. Let $\mathbf{Y}_{(k)}^{R,h}(\omega) \subset \mathbf{Y}_{(k)}^{R}(\omega)$ be the space of discretized test functions of dimension N_h.

Let now $\mathbf{B}^{k,h}(t) = \mathbf{B}_R^{k,h}(t) + \sum_{j=1}^{N_B} \mu_{B,j}^{k,h}(t)\,\mathbf{y}_{S,j}^{k,h}$ be the discrete solution. After discretization in space, the semi-discretized variational formulation is written (with the addition of the index ^{h}) in the same way as (6.1). It can be expressed equivalently as a linear system:

$$\frac{d^2}{dt^2}\mathbb{M}_{rr}B_R^k \;+\; \mathbb{M}_{rs}^k{\mu_B^k}'' \;+\; c^2\mathbb{K}_{rr}^k B_R^k \;=\frac{1}{\varepsilon_0}\mathbb{R}_{rr}^k J^k, \tag{6.2}$$
$$\frac{d^2}{dt^2}\mathbb{M}_{sr}^k B_R^k \;+\; \mathbb{M}_{ss}^k{\mu_B^k}'' \;+\; c^2\mathbb{K}_{ss}^k \mu_B^k \;=\frac{1}{\varepsilon_0}\mathbb{R}_{sr}^k J^k, \tag{6.3}$$

where $\mathbb{M}_{rr}$ denotes the mass matrix that does not depend to the Fourier mode k, $\mathbb{M}_{rs}^k$ is a (N_h, N_B) rectangular matrix coming from the integral over ω of the product of the N_B singular functions $\mathbf{y}_{S,j}^{k,h}$ by the basis functions of $\mathbf{Y}_{(k)}^{R,h}(\omega)$, $\mathbb{M}_{sr}^k$ being its transpose. Similarly, the matrix $\mathbb{K}_{rr}^k$ is associated to the term $a_k\left(\mathbf{B}_R^k(t),\mathbf{C}\right)\mathbb{R}_{rr}^k$ coming from the source term with $\mathbf{curl}\,_k\mathbf{J}^k$, and μ_B^k standing for the vector of $\mathbb{R}^{N_B}$ of entries $(\mu_{B,j}^k)$. Finally, $\mathbb{M}_{ss}^k$ and $\mathbb{K}_{ss}^k$ are the "singular" mass and stiffness matrices of dimension (N_B, N_B), associated to the term $\left(\mathbf{y}_{S,j}^k, \mathbf{y}_{S,i}^k\right)$ and $a_k\left(\mathbf{y}_{S,j}^k, \mathbf{y}_{S,i}^k\right)$ respectively. For these singular matrices, the computation must be carried out precisely in the neighborhood of the singularities by using a quadrature formula of high order.

We then perform a time discretization involving a second-order explicit (leap-frog) scheme. Here the notation X^n (resp. X^{n+1}) stands for a variable X at time $t^n = n\Delta t$ (resp. $t^{n+1} = (n+1)\Delta t$), where Δt is the time-step. F^n, G^n, H^n is the set of quantities known at time t^n for each equation of the

scheme (6.2)–(6.3), which can be rewritten as

$$\mathbb{M}_{rr} B_R^{k,n+1} + \mathbb{M}_{rs}^k \mu_B^{k,n+1} = F^{k,n}, \tag{6.4}$$

$$\mathbb{M}_{sr}^k B_R^{k,n+1} + \mathbb{M}_{ss}^k \mu_B^{k,n+1} = G^{k,n}. \tag{6.5}$$

To solve this linear system, a convenient way is to decouple $\mu_B^{k,n+1}$ and the unknown $B_R^{k,n+1}$as proposed in [5] for a two-dimensional Cartesian Maxwell system of equations, in the case of $N_B = 1$. The method developed here is more general, since it is also adapted to a domain with $N_B \geq 1$. For this purpose, we simply substitute (6.4)$-\mathbb{M}_{rs}^k(\mathbb{M}_{ss}^k)^{-1}$(6.5) to obtain a system where $\mu_B^{k,n+1}$ does no appear anymore. It remains now to invert this system to compute $B_R^{k,n+1}$, and then, at the corresponding time, the value $\mu_B^{k,n+1}$ by solving (6.5).

Compared to the system one would obtained in a regular domain, the additional effort is essentially the computation of the matrix $(\mathbb{M}_{ss}^k)^{-1}$. $\mathbb{M}_{ss}^k$ being a symmetric definite positive matrix (by construction) of dimension (N_B, N_B), i.e. a few units (and often $N_B = 1$), $(\mathbb{M}_{ss}^k)^{-1}$ is very easy to compute once and for all, for any mode k, $|k| \leq 2$.

For the sake of completeness, we conclude this section with a brief presentation of the electric case, that can be basically treat similarly to the magnetic case. Here, we consider the variational formulation (3.3) and also substitute the decomposition of the electric field (4.2) in regular and singular parts. Correspondingly, we add to the space of test functions $\mathbf{X}_{(k)}^R(\omega)$ the functions $(\mathbf{x}_{S,j}^k)_{j=1,N_E}$. Using again arguments of orthogonality, we obtain the following variational formulation:

Find $(\boldsymbol{E}_R^k, \boldsymbol{\mu}_E^k) \in \boldsymbol{X}_{(k)}^R(\omega) \times \mathbb{R}^{N_E}$ *such that*

$$\begin{cases} \left(\frac{\partial^2 \mathbf{E}_R^k(t)}{\partial t^2}, \mathbf{F}\right) + \sum_{j=1}^{N_E} (\mu_{E,j}^k)'' \left(\mathbf{x}_{S,j}^k, \mathbf{F}\right) + c^2\, a_k\left(\mathbf{E}_R^k(t), \mathbf{F}\right) \\ \quad = \quad -\frac{1}{\varepsilon_0}\left(\frac{\partial \mathbf{J}^k}{\partial t}, \mathbf{F}\right) + \frac{1}{\varepsilon_0}\left(\rho^k, \operatorname{div}_k \mathbf{F}\right), \quad \forall \mathbf{F} \in \mathbf{X}_{(k)}^R(\omega), \\ \left(\frac{\partial^2 \mathbf{E}_R^k(t)}{\partial t^2}, \mathbf{x}_{S,i}^k\right) + \sum_{j=1}^{N_E} (\mu_{E,j}^k)''\left(\mathbf{x}_{S,j}^k, \mathbf{x}_{S,i}^k\right) + c^2 \sum_{j=1}^{N_E} \mu_{E,j}^k(t)\, a_k\left(\mathbf{x}_{S,j}^k, \mathbf{x}_{S,i}^k\right) \\ \quad = \quad -\frac{1}{\varepsilon_0}\left(\frac{\partial \mathbf{J}^k}{\partial t}, \mathbf{x}_{S,i}^k\right) + \frac{1}{\varepsilon_0}\left(\rho^k, \operatorname{div}_k \mathbf{x}_{S,i}^k\right), \quad \forall \mathbf{x}_{S,i}^k \in \mathbf{X}_{(k)}^S(\omega). \end{cases}$$

From this variational formulation, the finite element approximation is defined by introducing the space of discretized test functions $\mathbf{X}_{(k)}^{R,h}(\omega) \subset \mathbf{X}_{(k)}^R(\omega)$. Here again, we choose P_2-conforming finite elements. Denoting

$$\mathbf{E}^{k,h}(t) = \mathbf{E}_R^{k,h}(t) + \sum_{j=1}^{N_E} \mu_{E,j}^{k,h}(t)\, \mathbf{x}_{S,j}^{k,h}$$

the discrete solution, we obtain the semi-discretized variational formulation,

that can be expressed by the following linear system:

$$\frac{d^2}{dt^2}\mathbb{M}_{rr}E_R^k \;+\; \mathbb{M}_{rs}^k {\mu_E^k}'' \;+\; c^2\mathbb{K}_{rr}^k E_R^k \;= -\frac{1}{\varepsilon_0}\frac{d}{dt}\mathbb{M}_{rr}J^k \;+\frac{1}{\varepsilon_0}\mathbb{L}_{rr}^k\rho^k,$$
$$\frac{d^2}{dt^2}\mathbb{M}_{sr}^k E_R^k \;+\; \mathbb{M}_{ss}^k {\mu_E^k}'' \;+\; c^2\mathbb{K}_{ss}^k \mu_E^k \;= -\frac{1}{\varepsilon_0}\frac{d}{dt}\mathbb{M}_{sr}^k J^k \;+\frac{1}{\varepsilon_0}\mathbb{L}_{sr}^k\rho^k\,.$$

The notations used being the same as for $\mathbf{B}^{k,h}(t)$, whereas the additional matrices $\mathbb{L}_{rr}^k$ and $\mathbb{L}_{sr}^k$ are associated to the term with divergence. As this system is very similar to (6.2)–(6.3), the time discretization is derived in the same way, and the solution is obtained correspondingly.

7 Numerical results

In this section, we present numerical results of singular field computations to illustrate the method. For the sake of simplicity, we will restrict ourselves to a domain with only one singular point. Hence, we will consider a 3-D top hat domain Ω with a reentrant circular edge, that corresponds, for a given θ, to an L-shaped 2-D domain ω with a reentrant corner. To compute the singular basis or time-dependent solutions, we introduce an unstructured mesh of ω made up of triangles, with no particular refinement near the reentrant corner. An example of such a mesh is presented in Figure 3.

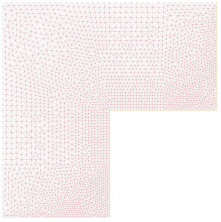

Figure 3. The typical mesh for a L-shaped domain ω.

We then approximate the variational formulations presented in the sections above by building a finite element method with FreeFem++ package [25], which implements a finite element method in space. As mentioned above, we recall that we actually used a P_2 finite element approximation in space, whereas the time discretization is performed by a second-order explicit scheme.

In addition, note that for a given geometry and for a given Fourier mode k, the singular bases $\mathbf{x}_{S,j}^k$ and $\mathbf{y}_{S,j}^k$ are computed during the initialization step, together with the additional regular-singular and singular-singular matrices like $\mathbb{M}_{rs}^k$ or $\mathbb{M}_{ss}^k$. More generally, the computational complexity of the algorithm basically depends on the orders of finite element and time discretization used, our approach can be used for a P_k finite element ($k \geq 1$), and for a time discretization scheme of order $p \geq 1$. For instance, if we denote by Q the number of quadrature points used for integration, the generation of the stiffness and mass matrix (need to be generated only once) are in $\mathcal{O}(QN_h)$. Similarly, assembling the element right-hand sides for $2N+1$ Fourier modes is in $\mathcal{O}((2N+1)QN_h)$

(N denoting the order of the truncated Fourier expansion, see (3.1)). The computational complexity also depends on the iterative method used for solving the final linear system of equations, that is the matrix $\mathbb{M}_{rr} - \mathbb{M}^k_{rs}(\mathbb{M}^k_{ss})^{-1}\mathbb{M}^k_{sr}$. However, for a chosen space and time-dependent method, in our case $k = 2$ and $p = 2$, we can evaluate the computational "additional effort" required by our discrete scheme, compared to the same scheme used in the standard way. Hence, the matrices $\mathbb{M}^k_{rs}, \mathbb{M}^k_{ss}$ and $\mathbb{M}^k_{sr}$ depend on the Fourier mode k, and the computational complexity of the assembling is in $\mathcal{O}(N_h)$. Further, updating the values of the singular coefficients $\mu^k_{E,j}(t)$ and $\mu^k_{B,j}(t)$ requires $O(1)$ operations per time-step. Therefore, the additional memory requirements, and computing effort, are relatively small, the complexity of the method and the memory requirements being better than that of the 3D methods.

Finally, it can be interesting to note what parts of subproblems can be solved in parallel. Clearly, the electric and magnetic problems can be solved separately (and so, in parallel), since we have considered Maxwell's equations written separately as two independent second-order wave equations. The singular basis $\mathbf{x}^k_{S,j}$ and $\mathbf{y}^k_{S,j}$, computed once for all, can be also solved in parallel, and independently for each singularity k. The time dependent part of the method can not be (easily) parallelized, for a given mode k, but since there is no coupling between the different modes (i.e., for different values of k), they can also be solved in parallel, as independent problems. and B are independent and can be solved separately. Basis x_s and y_s can also be solved separately, and also for each singularity.

7.1 Computation of the singular basis

We will present here, as an example, numerical results obtained in the computation of magnetic basis $\mathbf{y}^k_{S,j}$ for several values of k. The computation of the electric basis $\mathbf{x}^k_{S,j}$ can be dealt in a similar way.

As recalled in Proposition 1, it is sufficient to compute these basis only for the modes $k = -1, 0, 1, 2$, while the modes $k = 2$ or $k = -2$ will be use to compute all the higher modes $|k| > 2$. For this reason, we illustrate the computational method here by showing the numerical results obtained for these values of k. For this purpose, we follow the procedure presented in Section 5.

In Figure 4, we depicted the real part of the z-component for $\mathbf{y}^{-1}_S$ and $\mathbf{y}^0_S$, and the r-component for $\mathbf{y}^1_S$ and $\mathbf{y}^2_S$, obtained by solving the variational formulation (5.1), with a standard finite element method. Remember that they are complex quantities, as soon as $k \neq 0$. As one can see, the method is able to capture the singular behavior of the solution near the reentrant corner of ω (edge in Ω), whereas a conforming finite element method can not yield such a result. In addition, the results are not noisy, even though the mesh is not particularly refined near the edge.

Note that the mode $k = 0$ is a particular case that corresponds to the "fully" axisymmetric case. In [4, 8] we have proposed other ways to derive a method that can capture the singular solution. It is interesting (reassuring!) to note that the two approaches give the same results.

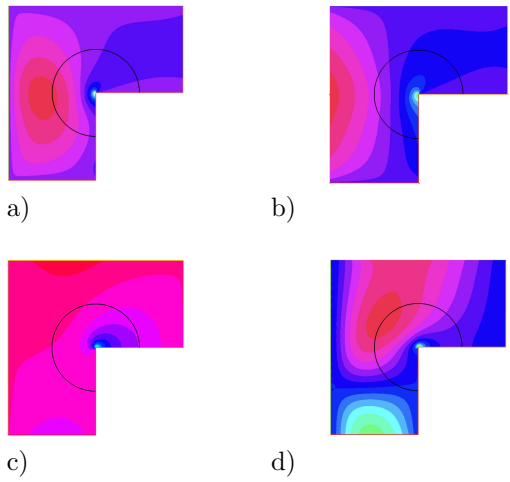

Figure 4. a) $\Re(\mathbf{y}^{-1}_{S,z})$, z-component of the singular basis for $k=-1$, b) $\mathbf{y}^{0}_{S,z}$, z-component of the singular basis for $k=0$, c) $\Re(\mathbf{y}^{1}_{S,r})$, r-component of the singular basis for $k=1$, d) $\Re(\mathbf{y}^{2}_{S,r})$, r-component of the singular basis for $k=2$.

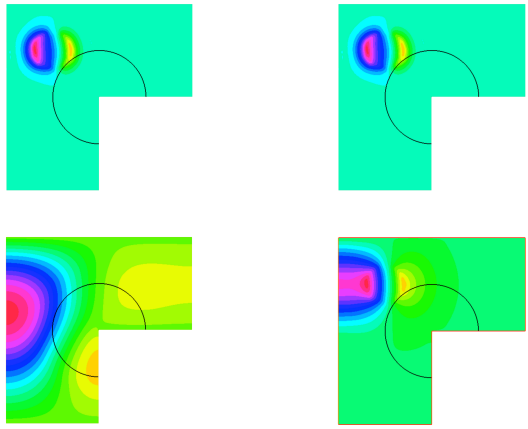

Figure 5. Case $k=0$ - Top: $\mathbf{B}^0(t_1)$ and $\mathbf{B}^0_R(t_1)$, for $t_1 < t_I$. Bottom: $\mathbf{B}^0(t_2)$ and $\mathbf{B}^0_R(t_2)$, for $t_2 > t_I$.

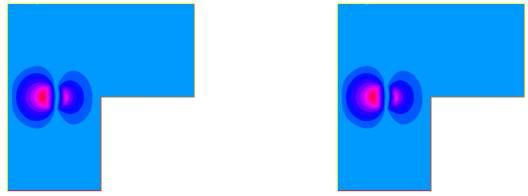

Figure 6. $\mathbf{B}^1(t_1)$ and $\mathbf{B}^1_R(t_1)$, for $t_1 < t_I$ (case $k=1$), z-component.

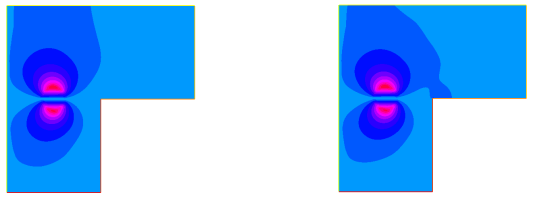

Figure 7. $\mathbf{B}^1(t_2)$ and $\mathbf{B}^1_R(t_2)$, for $t_2 > t_I$ (case $k = 1$), r-component.

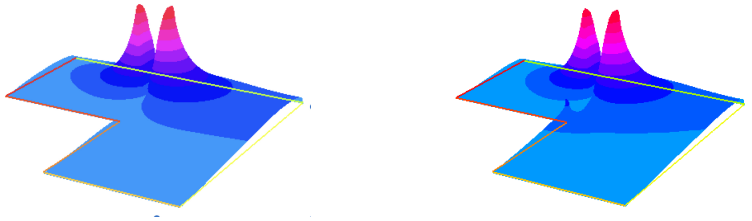

Figure 8. $\mathbf{B}^1(t_2)$ and $\mathbf{B}^1_R(t_2)$, for $t_2 > t_I$ (case $k = 1$), r-component.

7.2 Time-dependent case

This subsection is a follow-up of the previous one, to give an example of time-dependent case. Hence, we will concentrate on the magnetic case. We consider the same L-shaped domain ω as above, on which a perfectly conducting boundary condition is imposed, and we want to numerically compute $\mathbf{B}^k(t) = \mathbf{B}^k_R(t) + \mu^k_B(t)\mathbf{y}^k_S$, where, for each k, $\mu^k_B(t)$ is a smooth function in time and $\mathbf{y}^k_S$ is the singular basis already computed.

We are interested in computing the magnetic field $\mathbf{B}^k(t)$ created by a current loop. Then, initial conditions are set to zero, and a current is defined as $\mathbf{J}(t) = 10\sin(\lambda t)\mathbf{e}_\theta$, with a frequency $\lambda/2\pi = 2.5$GHz. The support of this current is a little disc centered around the middle of the domain. This current generates a wave which propagates circularly around the current source. Physically, as long as the wave has not reached the reentrant corner, the field is smooth.

Let t_I be the impact time, then, if one writes $\mathbf{B}^k(t) = \mathbf{B}^k_R(t) + \mu^k_B(t)\mathbf{y}^k_S$, $\mu^k_B(t) = 0$ for all t lower than t_I, and $\mathbf{B}^k(t)$ and $\mathbf{B}^k_R(t)$ coincide. On the other hand, for $t > t_I$, $\mu^k_B(t) \neq 0$ (and so $\mu^k_B(t)\mathbf{y}^k_S$ is) and the total field differs from its regular part.

This behavior is illustrated on Figures 5–8 for $k = 0$ and $k = 1$. Similar results are obtained for other values of k. Note that, for $|k| > 2$, the singular basis used is $\mathbf{y}^2_S$, as explained above.

8 Conclusions

In this article, we have presented a numerical method to solve the three-dimensional time-dependent Maxwell equations in a non-smooth and non con-

vex axisymmetric domain, with arbitrary data.

Using the axisymmetric assumption, the singular computational was reduced to a subset of $\mathbb{R}^2$, even if the electromagnetic field remain in $\mathbb{R}^3$. By performing a Fourier transform in the third dimension, the problem can be reduced to a sequence of singular problems set in a 2D domain.

Then, one has used a splitting of the space of solutions with respect to regularity, in a regular subspace, which is equal to the entire space of solutions when the domain is smooth or convex, and a singular subspace that has been characterized. Consequently, we have derived a variational formulation from which an original finite element numerical approach, based on standard Lagrange finite elements, was developed to solve these problems.

Numerical experiments have also been shown to illustrate that the method is able to capture the singular part of the solution. This approach can also be viewed as a generalized Singular Complement Method. Finally, note that this approach is easy to implement, as it can be included in already existing computational codes, without having to rewrite them entirely, and for a small additional computational cost.

References

[1] F. Assous, P. Ciarlet, Jr. and S. Labrunie. Theoretical tools to solve the axisymmetric Maxwell equations. *Math. Meth. Appl. Sci.*, **25**:49–78, 2002. https://doi.org/10.1002/mma.279.

[2] F. Assous, P. Ciarlet, Jr. and S. Labrunie. Solution of axisymmetric Maxwell equations,. *Math. Meth. Appl. Sci.*, **26**(10):861–896, 2003. https://doi.org/10.1002/mma.400.

[3] F. Assous, P. Ciarlet, Jr. and S. Labrunie. *Mathematical Foundations of Computational Electromagnetism.* Appl. Math. Sc., AMS 198, Springer, 2018. https://doi.org/10.1007/978-3-319-70842-3.

[4] F. Assous, P. Ciarlet, Jr., S. Labrunie and J. Segré. Numerical solution to the time-dependent Maxwell equations in axisymmetric singular domains: The singular complement method. *J. Comput. Phys.*, **191**(1):147–176, 2003. https://doi.org/10.1016/S0021-9991(03)00309-7.

[5] F. Assous, P. Ciarlet, Jr. and J. Segré. Numerical solution to the time-dependent Maxwell equations in two-dimensional singular domain: The singular complement method. *J. Comput. Phys.*, **161**(1):218–249, 2000. https://doi.org/10.1006/jcph.2000.6499.

[6] F. Assous, P. Degond, P.A. Raviart and J. Segré. On a finite element method for solving the three-dimensional Maxwell equations. *J. Comput. Phys.*, **109**(2):222–237, 1993. https://doi.org/10.1006/jcph.1993.1214.

[7] F. Assous, P. Degond and J. Segré. Numerical approximation of the Maxwell equations in inhomogeneous media by a p^1 conforming finite element method. *J. Comput. Phys.*, **128**(2):363–380, 1996. https://doi.org/10.1006/jcph.1996.0217.

[8] F. Assous and I. Raichik. Solving numerically the static Maxwell equations in an axisymmetric singular geometry. *Maths. Model. Anal.*, **20**(1):9–29, 2015. https://doi.org/10.3846/13926292.2015.996615.

[9] F. Assous and I. Raichik. Numerical solution to the 3D static Maxwell equations in axisymmetric singular domains with arbitrary data. *Comput. Meths. Applied Maths.*, **20**:419–435, 2020. https://doi.org/10.1515/cmam-2018-0314.

[10] F. Ben Belgacem, C. Bernardi and F. Rapetti. Numerical analysis of a model for an axisymmetric guide for electromagnetic waves. I. the continuous problem and its Fourier expansion. *Math. Methods Appl. Sci*, **28**(17):2007–2029, 2005. https://doi.org/10.1002/mma.649.

[11] F.Z. Belhachmi, C. Bernardi, S. Deparis and F. Hecht. A truncated Fourier/finite element discretization of the Stokes equations in an axisymmetric domain. *Math. Models Meth. App. Sci.*, **16**(2):233–263, 2006. https://doi.org/10.1142/S0218202506001133.

[12] C. Bernardi and Y. Maday. *Spectral methods for axisymmetric domains*. Series in Applied Mathematics, Gauthier-Villars, Paris and North Holland, Amsterdam, 1999.

[13] M.Sh. Birman and M.Z. Solomyak. L2-theory of the Maxwell operator in arbitrary domains. *Russian Math. Surveys*, **42**(6):75–96, 1987. https://doi.org/10.1070/RM1987v042n06ABEH001505.

[14] M.Sh. Birman and M.Z. Solomyak. The Weyl asymptotic decomposition of the spectrum of the Maxwell operator for domain with lipschitzian boundary. *Vestnik. Leningr. Univ. Math.*, **20**:15–21, 1987.

[15] S.C. Brenner, J. Gedicke and L.-Y. Sung. An adaptive P1 finite element method for two-dimensional Maxwell's equations. *Journal of Scientific Computing*, **55**:738–754, 2013. https://doi.org/10.1007/s10915-012-9658-8.

[16] C. Canuto, M.Y. Hussaini, A. Quarteroni and T. A. Zang. *Spectral Methods in Fluid Dynamics*. Springer-Verlag, New York, 1988. https://doi.org/10.1007/978-3-642-84108-8.

[17] Q. Chen and P. Monk. *Introduction to applications of numerical analysis in time domain computational electromagnetism*. Lecture Notes in Computational Science and Engineering, 2012. https://doi.org/10.1007/978-3-642-23914-4_3.

[18] P. Ciarlet, Jr., B. Jung, S. Kaddouri, S. Labrunie and J. Zou. The Fourier-singular complement method for Poisson equation. Part II: axisymmetric domains. *Numer. Math.*, **102**:583–610, 2006. https://doi.org/10.1007/s00211-005-0664-8.

[19] P. Ciarlet, Jr. and S. Labrunie. Numerical solution of Maxwell's equations in axisymmetric domains with the Fourier singular complement method. *Diff. Eq. & Applic.*, **3-1**:113–155, 2011.

[20] D.M. Copeland, J. Gopalakrishnan and J.E. Pasciak. A mixed method for axisymmetric div-curl systems. *Math. Comp.*, **77**:1941–1965, 2008. https://doi.org/10.1090/S0025-5718-08-02102-9.

[21] M. Costabel. A remark on the regularity of solutions of Maxwell's equations on Lipschitz domains. *Math. Meth. Appl. Sci.*, **12**(4):365–368, 1990. https://doi.org/10.1002/mma.1670120406.

[22] M. Costabel, M. Dauge and S. Nicaise. Singularities of Maxwell interface problems. *Model. Math. Anal. Num.*, **33**(3):627–649, 1999. https://doi.org/10.1051/m2an:1999155.

[23] P. Grisvard. *Elliptic problems in nonsmooth domains, Monographs and Studies in Mathematics*. Pitman, London, 1985.

[24] P. Grisvard. *Singularities in boundary value problems.* RMA 22, Masson, Paris, 1992.

[25] F. Hecht. New development in FreeFem++. *J. Numer. Math.*, **20**(3-4):251–265, 2012. https://doi.org/10.1515/jnum-2012-0013.

[26] B. Heinrich. The Fourier-finite element method for Poisson's equation in axisymmetric domains with edges. *SIAM J. Numer. Anal.*, **33**(5):1885–1911, 1996. https://doi.org/10.1137/S0036142994266108.

[27] B. Heinrich, S. Nicaise and B. Weber. Elliptic interface problems in axisymmetric domains II: Convergence analysis of the Fourier-finite element method. *Adv. Math. Sci. Appl.*, **10**:571–600, 2003.

[28] J.S.Hestaven and T.Warburton. *Nodal discontinuous Galerkin methods.* Texts in Applied Mathematics, Springer, 2008. https://doi.org/10.1007/978-0-387-72067-8.

[29] J.L. Lions and E. Magenes. *Non-Homogeneous Boundary Value Problems and Applications, vol. I.* Springer, 1972. https://doi.org/10.1007/978-3-642-65161-8.

[30] B. Mercier and G. Raugel. Resolution d'un probleme aux limites dans un ouvert axisymétrique par élément finis en r, z et séries de Fourier en θ. *R.A.I.R.O. Anal. numér.*, **16**:405–461, 1982. https://doi.org/10.1051/m2an/1982160404051.

[31] J-C. Nédelec. Mixed finite elements in R^3. *Numer. Math.*, **35**:315–341, 1980. https://doi.org/10.1007/BF01396415.

[32] J-C. Nédelec. A new family of mixed finite elements in R^3. *Numer. Math.*, **50**:57–81, 1986. https://doi.org/10.1007/BF01389668.

[33] B. Nkemzi. Optimal convergence recovery for the Fourier-finite-element approximation of Maxwell's equations in nonsmooth axisymmetric domains. *Numer. Math.*, **57**:989–1007, 2007. https://doi.org/10.1016/j.apnum.2006.09.006.

[34] C. Weber. A local compactness theorem for Maxwell's equations. *Math. Meth. Appl. Sci.*, **2**(1):12–25, 1980. https://doi.org/10.1002/mma.1670020103.